



# HHS Public Access

Author manuscript

*Neurobiol Dis.* Author manuscript; available in PMC 2016 August 01.

Published in final edited form as:

*Neurobiol Dis.* 2015 August ; 80: 70–79. doi:10.1016/j.nbd.2015.04.016.

## Inflammatory mechanisms contribute to the neurological manifestations of tuberous sclerosis complex

Bo Zhang, Jia Zou, Nicholas R Rensing, Meihua Yang, and Michael Wong

Department of Neurology and the Hope Center for Neurological Disorders, Washington University School of Medicine, St. Louis, Missouri, USA

### Abstract

Epilepsy and other neurological deficits are common, disabling manifestations of the genetic disorder, Tuberous Sclerosis Complex (TSC). Brain inflammation has been implicated in contributing to epileptogenesis in acquired epilepsy due to brain injury, but the potential role of inflammatory mechanisms in genetic epilepsies is relatively unexplored. In this study, we investigated activation of inflammatory mediators and tested the effects of anti-inflammatory treatment on epilepsy in the *Tsc1*-GFAP conditional knock-out mouse model of TSC (*Tsc1*<sup>GFAP</sup>CKO mice). Real-time quantitative RT-PCR, immunohistochemistry, and western blotting demonstrated increased expression of specific cytokines and chemokines, particularly IL-1 $\beta$  and CXCL10, in the neocortex and hippocampus of *Tsc1*<sup>GFAP</sup>CKO mice, which was reversed by treatment with a mammalian target of rapamycin complex 1 (mTORC1) inhibitor. Double-labeling immunohistochemical studies indicated that the increased IL-1 $\beta$  was localized primarily to astrocytes. Importantly, the increase in inflammatory markers was also observed in astrocyte culture *in vitro* and at 2 weeks of age in *Tsc1*<sup>GFAP</sup>CKO mice before the onset of epilepsy *in vivo*, indicating that the inflammatory changes were not secondary to seizures. Epicatechin-3-gallate, an inhibitor of IL-1 $\beta$  and CXCL10, at least partially reversed the elevated cytokine and chemokine levels, reduced seizure frequency, and prolonged survival of *Tsc1*<sup>GFAP</sup>CKO mice. These findings suggest that mTOR-mediated inflammatory mechanisms may be involved in epileptogenesis in the genetic epilepsy, TSC.

### Keywords

epilepsy; seizure; tuberous sclerosis; inflammation; mice; interleukin; cytokine; chemokine

---

© 2015 Published by Elsevier Inc.

Corresponding Author: Michael Wong, MD, PhD, Department of Neurology, Box 8111, Washington University School of Medicine, 660 South Euclid Avenue, St. Louis, MO 63110, Phone: 314-362-8713, Fax: 314-362-9462, wong\_m@wustl.edu.

**Publisher's Disclaimer:** This is a PDF file of an unedited manuscript that has been accepted for publication. As a service to our customers we are providing this early version of the manuscript. The manuscript will undergo copyediting, typesetting, and review of the resulting proof before it is published in its final citable form. Please note that during the production process errors may be discovered which could affect the content, and all legal disclaimers that apply to the journal pertain.

## INTRODUCTION

Tuberous sclerosis complex (TSC) is a genetic disorder, characterized by tumor or hamartoma formation in multiple organs (Crino et al., 2006; Orlova and Crino, 2010). Neurological involvement often accounts for the most disabling symptoms of TSC, including drug-resistant epilepsy, intellectual disability, and autism (Chu-Shore et al., 2010; Holmes et al., 2007). TSC is caused by mutations in the *TSC1* or *TSC2* genes, which leads to hyperactivation of the mammalian target of rapamycin complex 1 (mTORC1) pathway and stimulates cell growth and proliferation, promoting tumor growth. The use of mTOR inhibitors represents a rational, proven approach for treating tumors in TSC (Franz et al., 2013; Krueger et al., 2010).

Although TSC patients can develop brain tumors, the chronic neurological symptoms of epilepsy, intellectual disability, and autism are generally not directly caused by tumor growth per se. Cortical tubers, which represent static, developmental malformations or hamartomas of the brain, may contribute to some of the chronic neurological manifestations of TSC, especially epilepsy. However, there is also accumulating evidence that non-tuber, structurally normal-appearing regions of the brain possess cellular and molecular abnormalities that promote neurological dysfunction (Wong, 2008).

Independent of tumor growth, the mTORC1 pathway has also been implicated in promoting epilepsy and intellectual disability in TSC patients, and mTOR inhibitors are being tested in clinical trials as potential treatments for these neurological symptoms (Krueger et al., 2013). Even if mTOR inhibitors are effective against neurological manifestations of TSC, the critical mechanisms downstream from mTORC1 causing epilepsy and neurocognitive dysfunction in TSC are poorly understood. As mTORC1 inhibitors have significant side effects, such as immunosuppression, identification of these downstream mechanisms may lead to more targeted therapies, with more specific efficacy and fewer side effects.

Brain inflammation has been strongly implicated in the pathophysiology of epilepsy and other neurological disorders (Vezzani et al., 2013a, 2013b; Xu et al., 2013). While activation of inflammatory mechanisms in response to acquired brain injury is perhaps not surprising, a more novel idea is that brain inflammation could also be important in the pathophysiology of developmental or genetic neurological disorders. In fact, inflammatory markers, such as cytokines and chemokines, have been found in brain specimens from patients with genetic malformations of cortical development, including TSC (Boer et al., 2008, 2010; Maldonado et al., 2003; Prabowo et al., 2013), but the pathophysiological significance of inflammation in TSC is poorly understood. Thus, the purpose of this study is to identify specific inflammatory mechanisms, downstream from mTOR, activated in the brain of a mouse model of TSC and determine the effect of modulating these mechanisms.

## MATERIALS AND METHODS

### Animals and drug treatment

Care and use of animals were conducted according to an animal protocol approved by the Washington University Animal Studies Committee. *Tsc1*<sup>flox/flox</sup>-GFAP-Cre knock-out

(*Tsc1*<sup>GFAPCKO</sup>) mice with conditional inactivation of the *Tsc1* gene predominantly in glia were generated as described previously (Uhlmann et al., 2002). *Tsc1*<sup>flox/+</sup>-GFAP-Cre and *Tsc1*<sup>flox/flox</sup> littermates have previously been found to have no abnormal phenotype and were used as control animals in these experiments.

In some experiments, three-week-old *Tsc1*<sup>GFAPCKO</sup> mice were treated with rapamycin (3 mg/kg/day) or vehicle for one week, and brain tissues were then harvested for western blot, real-time quantitative RT-PCR, or immunohistochemistry analysis. Rapamycin (LC Labs, Woburn, MA) was initially dissolved in 100% ethanol, stored at -20°C, and diluted in a vehicle solution containing 5% Tween 80, 5% PEG 400 (Sigma, St. Louis, MO), and 4% ethanol immediately before injection or adding to the culture medium.

In other experiments, three-week-old *Tsc1*<sup>GFAPCKO</sup> mice were treated with vehicle (saline) or Epicatechin-3-gallate (ECG, Sigma, St Louis, MO). ECG dissolved in saline was administered by peritoneal injection at the dose of 12.5 mg/kg/d for one week for western blot and immunohistochemistry analysis, for four weeks for histology, and for up to 12 weeks for video-EEG monitoring. Vehicle-treated non-KO littermates served as additional controls. Other vehicle or ECG-treated *Tsc1*<sup>GFAPCKO</sup> mice and control mice were monitored for body and brain weight measurements or for survival analysis.

### Real-time Quantitative RT-PCR

Real-time quantitative RT-PCR was used to screen a panel of inflammatory markers (Table S1). Total RNA was prepared from brain of two or four week old *Tsc1*<sup>GFAPCKO</sup> or control mice, or from cultured astrocytes of *Tsc1*<sup>GFAPCKO</sup> or control mice. Following DNase I treatment (Invitrogen, Grand Island, NY), cDNA was synthesized using iScript Reverse Transcription Kit (BIO-RAD, Hercules, CA). The following conditions were used for reverse transcription: 25°C for 10 min, 48°C for 30 min, and 95°C for 5 min.

Each 25 µl PCR contained 2 µl cDNA, 12.5 µl of 2X SYBR Green PCR Master Mix (Applied Biosystems, Foster city, CA), and 12.5 pmol of each primer. Real-time quantitative PCR was performed in 96-well optical reaction plates on the AB1 7000 Real-Time PCR System (Applied Biosystems) under the following conditions: 50°C for 2 min, 95°C for 10 min, and then 40 cycles of 95°C for 15 s and 60°C for 1 min. Emitted fluorescence for each reaction was measured at the annealing/extension phase. All oligonucleotide primers used for quantitative PCR were designed using Primer Express v2.0 (Applied Biosystems). Calculated copies were normalized against copies of the housekeeping gene glyceraldehyde-3-phosphate dehydrogenase (GAPDH). Forward and reverse primer sets are listed in Table S1.

### Western blotting

Western blot analysis was used to measure protein levels of CXCL10 in the brains of *Tsc1*<sup>GFAPCKO</sup> mice, using standard methods as described previously (Zeng et al., 2008). Briefly, brains were dissected and homogenized separately. Equal amounts of total protein extract were separated by gel electrophoresis and transferred to nitrocellulose membranes. β-actin was used as a loading control. After incubating with primary antibodies to CXCL10

(1:1,000; Abcam, Cambridge, MA), or  $\beta$ -actin (1:2,000; Cell Signaling Technology), the membranes were reacted with a peroxidase-conjugated secondary antibody (1:1,000, Cell Signaling Technology). Signals were detected by enzyme chemiluminescence (GE healthcare life science, Little Chalfont Buckinghamshire, UK) and quantitatively analyzed with ImageJ software (NIH, Bethesda, MD).

### Immunohistochemistry/Histology

Histological analysis was performed to assess glial proliferation and neuronal organization by standard methods, as previously described (Zeng et al., 2008). In brief, brains were perfusion-fixed with 4% paraformaldehyde and cut into 45  $\mu$ m sections with a cryotome. Some sections were stained with 0.5% cresyl violet. Other sections were labeled with GFAP antibody (anti-GFAP, mouse; 1:500; Cell Signaling Technology, Beverly, MA), and then Cy3-conjugated goat anti-mouse IgG (1:500; Jackson Immuno. West Grove, PA).

In other experiments, immunohistochemistry was performed for IL-1 $\beta$ , by labeling with primary antibody (anti-IL-1 $\beta$ , rabbit, 1:500; Abcam), followed by labeling with secondary antibody Alexa-488 conjugated goat anti-rabbit IgG (1:500; Life Technologies, Grand Island, NY). Some sections were double stained with GFAP antibody (anti-GFAP, mouse; 1:500; Cell Signaling Technology), NeuN antibody (anti-NeuN, mouse, 1:500; Millipore, Billerica, MA), or Iba1 antibody (anti-Iba1, mouse, 1:500; Millipore), followed by labeling with secondary antibodies: Alexa-488 conjugated goat anti-rabbit IgG (1:500; Life Technologies, Grand Island, NY) or Cy3 conjugated goat anti-mouse IgG (1:500; Jackson Immuno, West Grove, PA). In addition, some sections were counterstained with TO-PRO-3 Iodide (1:1,000; Life Technologies) for the nonspecific nuclear staining of all cells.

For blinded analysis, images were acquired with a Zeiss LSM PASCAL confocal microscope (Zeiss Thornwood, NY), or with a Nanozoomer HT system (Hamamatsu, Bridgewater, NJ). In images from coronal sections at approximately 2 mm posterior to bregma and approximately 1 mm from midline, regions of interest were marked in neocortex by a 200 $\mu$ m-wide box spanning from the neocortical surface to the bottom of layer VI and in hippocampus by areas up to 0.04 mm<sup>2</sup> within the striatum radiatum of CA1 and dentate gyrus. GFAP-immunoreactive cells were quantified in the regions of interest from two sections per mouse from a total of eight mice per group. Similarly, IL-1 $\beta$  positive cells and TO-PRO-3 Iodide stained cells numbers were counted in the sections of each groups, and IL-1 $\beta$  positive cell numbers were normalized to TO-PRO-3 Iodide stained cell number, and were presented as IL-1 $\beta$  positive cells/100 TO-PRO-3 positive cells.

### ELISA of serum IL-1 $\beta$ and CXCL10 expression

IL-1 $\beta$  and CXCL10 proteins were assayed in duplicate from serum of four week old *Tsc1*<sup>GFAP</sup>CKO mice and control mice with the mouse IL-1 $\beta$  and CXCL10 enzyme-linked immunosorbent assay (ELISA) kits (R&D System, Minneapolis, MN, USA) according to the manufacturer's instructions. Additional control mice were treated with lipopolysaccharide (LPS, 250  $\mu$ g/kg, i.p.), as a positive control. Blood was collected 6 h following i.p. LPS administration and serum was separated from clotted blood overnight at 4 °C

### Astrocyte culture and measurement of inflammatory markers in vitro

Astrocytes were obtained from mixed cell cultures of the forebrains as described previously (Zhang et al., 2002), with slight modification to remove microglial cells completely. Briefly, the forebrains of newborn *Tsc1*<sup>GFAP</sup>CKO mice and non-KO littermates were dissected and the dissociated brain cells were seeded in a poly-D-lysine-coated 75 cm<sup>2</sup>-culture flask (Becton Dickinson Labware, Franklin Lakes, NJ). Cells were cultured for 8–10 days until confluent, then they were vigorously hand-shaken for 0.5–1 min to remove microglial cells present on the astrocyte monolayer, followed by medium exchange and incubation overnight in a CO<sub>2</sub> incubator. The purification procedure was repeated three times during the subsequent 3 days. Finally, the flask was washed with DMEM several times and the medium replaced with Neurobasal medium for 6 hours before treatment.

Rapamycin at a concentration of 2 ng/ml or vehicle were added to the medium of prepared astrocytes and incubated for 16 hours. Samples were collected after trypsinization with 0.25% trypsin-EDTA (Invitrogen, Grand Island, NY), and then Western blotting analysis was performed to measure the ratio of CXCL10 and  $\beta$ -actin as described above, or real-time RT-PCR was used to measure the mRNA level of CCL2, IL-1 $\beta$  and CXCL10.

### Video-electroencephalography monitoring

Vehicle- and ECG-treated *Tsc1*<sup>GFAP</sup>CKO mice underwent continuous video-EEG monitoring starting at 3 weeks of age, using established methods for implanting epidural electrodes and performing continuous video-EEG recordings, as described previously (Erbayat-Altay et al., 2007; Zeng et al., 2008). Briefly, mice were anesthetized with isoflurane and placed in a stereotaxic frame. Epidural screw electrodes were surgically implanted and secured using dental cement for long term EEG recordings. Four electrodes were placed on the skull: one right and one left central electrodes (1 mm lateral to midline, 2 mm posterior to bregma), one frontal electrode (0.5 mm anterior and 0.5 mm to the right or left of bregma) and one occipital electrode (0.5 mm posterior and 0.5 mm to the right or left lambda). The typical recording montage involved two EEG channels with the right and left central “active” electrodes being compared to either the frontal or occipital “reference” electrode. Video and EEG data were acquired simultaneously with an AD Instruments PowerLab video-EEG system. Continuous 24/7 video-EEG data were obtained every week from each mouse, for the life of the animal or until 12 weeks of age, and were analyzed for seizures. Electrographic seizures were identified by their characteristic pattern of discrete periods of rhythmic spike discharges that evolved in frequency and amplitude lasting at least 10 seconds, typically ending with repetitive burst discharges and voltage suppression. On video analysis, the behavioral correlate to these seizures typically involved head bobbing, rearing with forelimb clonus, and occasional generalized convulsive activity. Seizure frequency (number of seizures per week period, based on analysis of the entire EEG record) was calculated from each week epoch.

### Statistics

All statistical analysis was performed using GraphPad Prism (GraphPad Software). Quantitative differences between groups were analyzed by Student's *t* test or one-way ANOVA with Turkey's multiple comparisons post hoc tests when comparing one factor

over more than two groups or by repeated measures two-way ANOVA when comparing multiple treatment variables (e.g. effect of treatment and genotype). Comparable non-parametric tests were used when data did not fit a normal distribution. Chi-Square test was used for survival analysis. Quantitative data are expressed as mean  $\pm$  SEM. Statistical significance was defined as  $p < 0.05$ .

## RESULTS

### Proinflammatory cytokines and chemokines are up-regulated in *Tsc1*<sup>GFAP</sup>CKO mice and inhibited by rapamycin

We first used real-time quantitative RT-PCR to screen for inflammatory markers activated in *Tsc1*<sup>GFAP</sup>CKO mice. The mRNA levels of CCL2, IL-1 $\beta$ , IFN- $\gamma$ , CXCL10 and IL-6 were increased in the brains of four-week-old *Tsc1*<sup>GFAP</sup>CKO mice compared to control mice, while the mRNA level of CXCL12 was decreased (Fig. 1A). As seizures in *Tsc1*<sup>GFAP</sup>CKO mice start around 3–4 weeks of age (Erbayat-Altay et al., 2007; Zeng et al., 2011) and could secondarily affect inflammation, we then performed real-time quantitative RT-PCR in two-week old *Tsc1*<sup>GFAP</sup>CKO mice. Only the mRNA levels of CCL2, IL-1 $\beta$ , and CXCL10 were increased in two-week-old *Tsc1*<sup>GFAP</sup>CKO mice compared to control mice; no significant difference was found in IFN- $\gamma$ , IL-6 and CXCL12 in two-week-old *Tsc1*<sup>GFAP</sup>CKO mice (Fig. 1B). Similar to the results of two-week-old mice, the mRNA levels of CCL2, IL-1 $\beta$ , and CXCL10 were increased in the cultured astrocytes of *Tsc1*<sup>GFAP</sup>CKO mice compared to the astrocytes of control mice (Fig. 1C).

To assess whether mTOR activation may be involved in the upregulation of inflammatory markers in *Tsc1*<sup>GFAP</sup>CKO mice, we tested the effect of rapamycin on mRNA levels of those markers that were consistently elevated in the previous experiments. Rapamycin treatment at the dose of 3 mg/kg/d for seven days significantly inhibited the mRNA levels of CCL2, IL-1 $\beta$  and CXCL10 in the brains of *Tsc1*<sup>GFAP</sup>CKO mice in vivo compared with vehicle treated *Tsc1*<sup>GFAP</sup>CKO mice (Fig. 1D). For in vitro experiments, treatment of astrocytes with rapamycin at the dose of 2 ng/ml, down-regulated the mRNA expression of CCL2 and CXCL10, although the effect on IL-1 $\beta$  did not reach significance (Fig. 1E).

### IL-1 $\beta$ protein is upregulated in *Tsc1*<sup>GFAP</sup>CKO mice and inhibited by anti-inflammatory treatments

We next tested whether inflammatory markers increased on the mRNA level translated to upregulated protein in *Tsc1*<sup>GFAP</sup>CKO mice. Immunohistochemistry of IL-1 $\beta$  was performed in brain sections of four-week old mice treated with vehicle, rapamycin, or ECG for one week starting at three weeks of age. IL-1 $\beta$  protein expression was strongly detected in hippocampal brain sections of *Tsc1*<sup>GFAP</sup>CKO mice (Fig. 2B, E), but rarely in control mice (Fig. 2A, D). Treatment with rapamycin (3 mg/kg/d i.p.) significantly inhibited the IL-1 $\beta$  expression in *Tsc1*<sup>GFAP</sup>CKO mice (Fig. 2C, F, I). Epicatechins have been reported to inhibit IL-1 $\beta$  and CXCL10 expression (Crouvezier et al., 2001; Hosokawa et al., 2010). ECG treatment (12.5 mg/kg/d i.p) also inhibited expression of IL-1 $\beta$  expression in *Tsc1*<sup>GFAP</sup>CKO mice (Fig. 2G, H, I).

To define the cellular localization of IL-1 $\beta$ , we double labeled sections with three different combinations of double immunofluorescence staining: IL-1 $\beta$  with GFAP for astrocytes (Fig. 2J), with NeuN for neurons (Fig. 2K) and with Iba1 for microglia (Fig. 2L). IL-1 $\beta$  colocalized with GFAP positive cells, but not with NeuN or Iba1 positive cells in the brains of four-week-old *Tsc1*<sup>GFAP</sup>CKO mice.

### **CXCL10 protein is upregulated in *Tsc1*<sup>GFAP</sup>CKO mice and reversed by anti-inflammatory treatment in vivo and in vitro**

Western blot analysis was used to measure protein levels of CXCL10. CXCL10 was increased in the brains of four-week-old *Tsc1*<sup>GFAP</sup>CKO mice compared to control mice (Fig. 3A), as well as in cultured astrocytes from *Tsc1*<sup>GFAP</sup>CKO mice (Fig. 3B). Rapamycin treatment at the dose of 3 mg/kg/d significantly reversed the up-regulated protein levels of CXCL10 in the brain of the four-week-old *Tsc1*<sup>GFAP</sup>CKO mice in vivo, compared with vehicle treated *Tsc1*<sup>GFAP</sup>CKO mice (Fig. 3A). Similarly, rapamycin treatment at the dose of 2 ng/ml for 16 hours, down-regulated the protein level of CXCL10 in cultured astrocytes of *Tsc1*<sup>GFAP</sup>CKO mice compared to vehicle treated astrocytes of *Tsc1*<sup>GFAP</sup>CKO mice (Fig. 3B). Furthermore, ECG treatment at the dose of 12.5 mg/kg/d started at the age of three weeks for seven days, significantly down-regulated the protein levels of CXCL10 in the brains of *Tsc1*<sup>GFAP</sup>CKO mice compared to vehicle-treated *Tsc1*<sup>GFAP</sup>CKO mice (Fig. 3C).

### **Lack of evidence of peripheral inflammation in *Tsc1*<sup>GFAP</sup>CKO mice**

In other models of epilepsy, systemic inflammation and breakdown of the blood-brain barrier may promote brain inflammation. In *Tsc1*<sup>GFAP</sup>CKO mice, the targeted genetic manipulation of *Tsc1* gene inactivation in GFAP-expressing cells in the brain and the demonstration of inflammatory markers in cultured cells in vitro make this possibility unlikely, especially as an early event before seizure onset. However, to investigate the potential contribution of systemic inflammatory factors in *Tsc1*<sup>GFAP</sup>CKO mice, serum expression of inflammatory markers was assessed. Although lipopolysaccharide injection in control mice caused an expected increase in serum IL-1 $\beta$  and CXCL10 levels assayed by ELISA, 4 week old *Tsc1*<sup>GFAP</sup>CKO mice had no increase in these inflammatory markers in the serum (Fig. 4A, B). Thus, the early inflammatory changes observed in the brains of *Tsc1*<sup>GFAP</sup>CKO mice are most likely due to modulation of innate brain immunity, not infiltration of peripheral immune mediators.

### **ECG treatment slightly decreases brain weight and glial proliferation, but does not affect body weight or neuronal organization of *Tsc1*<sup>GFAP</sup>CKO mice**

The effect of rapamycin on pathological abnormalities and epilepsy has been previously reported (Zeng et al., 2008). We similarly tested the effects of anti-inflammatory treatment with ECG on the neurological phenotype of *Tsc1*<sup>GFAP</sup>CKO mice. Consistent with previous studies (Uhlmann et al., 2002; Zeng et al., 2008), vehicle-treated *Tsc1*<sup>GFAP</sup>CKO mice developed dramatic, diffuse megalencephaly (brain weight = 519.0 $\pm$ 10.6 mg at 7 weeks of age) compared with non-KO control mice (389.2 $\pm$ 3.2 mg;  $p$ <0.001). ECG treatment at the dose of 12.5 mg/kg/d for four weeks slightly improved the megalencephaly in *Tsc1*<sup>GFAP</sup>CKO mice (485.0 $\pm$ 8.7;  $p$ <0.05 compared with vehicle-treated *Tsc1*<sup>GFAP</sup>CKO

mice). At 7 weeks of age, there was a trend towards a decrease in body weight in vehicle-treated *Tsc1*<sup>GFAP</sup>CKO mice (15.7±0.5 g) compared with non-KO control mice (18.3±0.9 g). ECG treatment had no significant effect on body weight of *Tsc1*<sup>GFAP</sup>CKO mice (14.9±0.8 g).

*Tsc1*<sup>GFAP</sup>CKO mice exhibit a progressive excessive glial proliferation (Uhlmann et al. 2002; Zeng et al., 2008). Consistent with previous studies, vehicle-treated *Tsc1*<sup>GFAP</sup>CKO mice showed a large increase in GFAP-positive cells in neocortex and hippocampus compared with non-KO control mice (Fig. 5A). ECG treatment at the dose of 12.5 mg/kg/d for four weeks caused a significant decrease in the number of GFAP positive cells in neocortex and dentate gyrus, but not in CA1 of hippocampus, of *Tsc1*<sup>GFAP</sup>CKO mice (Fig. 5B, C).

*Tsc1*<sup>GFAP</sup>CKO mice exhibit disorganization and dispersion of the pyramidal cell layer of hippocampus (Uhlmann et al., 2002; Zeng et al., 2008). Consistent with previous studies, Cresyl violet staining demonstrated that vehicle-treated *Tsc1*<sup>GFAP</sup>CKO mice had widely dispersed pyramidal cell layers (Fig. 6B) in all regions of hippocampus (CA1–CA4) compared with control mice (Fig. 6A). ECG treatment had no apparent effect on this neuronal disorganization in *Tsc1*<sup>GFAP</sup>CKO mice (Fig. 6C). Quantitative analysis showed a significant increase in the width of the CA1 pyramidal layer in vehicle-treated *Tsc1*<sup>GFAP</sup>CKO mice (114.8 ± 1.6 μm) compared with control mice (67.0 ± 2.4 μm; p<0.001 by one-way ANOVA, n=8 mice/group), but no effect of ECG in *Tsc1*<sup>GFAP</sup>CKO mice (109.8 ± 0.9 μm).

### **ECG treatment moderately decreases the development of seizures and improves survival in *Tsc1*<sup>GFAP</sup>CKO mice**

*Tsc1*<sup>GFAP</sup>CKO mice develop progressive epilepsy starting around three to four weeks of life and then die prematurely by around seven to ten weeks of age (Erbayat-Altay et al, 2007; Zeng et al., 2011). In the present study, video-EEG monitoring again showed that seizures developed in vehicle-treated *Tsc1*<sup>GFAP</sup>CKO mice around 3–5 weeks of life (3.6±2.1 seizures/week at 3 weeks) and became progressively more frequent with age (19.6±14.7 at 7 weeks). ECG treatment (12.5 mg/kg/d i.p.) caused a small, but significant decrease in seizure frequency in *Tsc1*<sup>GFAP</sup>CKO mice (Fig. 7A). However, all mice had at least one seizure in both vehicle-treated and ECG-treated *Tsc1*<sup>GFAP</sup>CKO mice.

Survival analysis confirmed previous studies demonstrating that vehicle-treated *Tsc1*<sup>GFAP</sup>CKO mice die prematurely, with 50% mortality between six to seven weeks of age and 100% mortality by ten weeks of age. ECG treatment caused a significant increase in survival of *Tsc1*<sup>GFAP</sup>CKO mice compared to vehicle-treated *Tsc1*<sup>GFAP</sup>CKO mice; all animals survived to seven weeks of age, and 50% of mice still survived at nine weeks of age. However, all ECG-treated mice eventually died by twenty weeks of age (Fig. 7B).

## **DISCUSSION**

TSC is one of the most common single-gene disorders causing drug-resistant epilepsy, intellectual disability, and autism. Proinflammatory mechanisms have been implicated in



contributing to the pathophysiology of epilepsy, especially acquired epilepsy due to brain injury. However, the role of brain inflammation in developmental or genetic epilepsies is relatively unexplored. In this study, we provide evidence that inflammatory signaling mechanisms, particularly the cytokine IL-1 $\beta$  and chemokine CXCL10, are abnormally activated in a mouse model of TSC. These inflammatory mediators were reversed by the mTORC1 inhibitor, rapamycin, indicating that these mechanisms are downstream from mTORC1, and occurred in astrocyte culture *in vitro* and before epilepsy onset *in vivo*, indicating that these changes were not secondary to seizures. Furthermore, inhibition of IL-1 $\beta$  and CXCL10 by ECG at least partially reduced seizure frequency and prolonged survival of *Tsc1*<sup>GFAP</sup>CKO mice, suggesting a potential role of anti-inflammatory treatments for epilepsy and other neurological manifestations in TSC.

Mechanisms of epileptogenesis in TSC are still poorly understood. In many cases, epilepsy may be caused by the focal malformations of cortical development, the tubers, which are the pathological hallmarks of TSC. However, beyond tubers, a variety of cellular and molecular abnormalities have been implicated in epileptogenesis in mouse models of TSC and pathological specimens from TSC patients (Wong, 2008). Independent of tumor growth, the mTORC1 pathway may regulate specific cellular and molecular mechanisms of epileptogenesis, such as neuronal death, synaptic reorganization, and expression of ion channels and neurotransmitter receptors (Wong, 2010, 2013). mTORC1 inhibitors can prevent the development of epilepsy and inhibit ongoing seizures in mouse models of TSC (Goto et al., 2011; Meikle et al., 2008; Zeng et al., 2008, 2011), as well as in some models of acquired epilepsy due to brain injury (Berdichevsky et al., 2013; Guo et al., 2013; Huang et al., 2010; van Vliet et al., 2012; Zeng et al., 2009). Preliminary clinical trials suggest that mTOR inhibitors may be effective in reducing seizures in TSC patients with refractory epilepsy (Krueger et al., 2013). Even if mTOR plays a critical role in epilepsy in TSC, the specific mechanisms downstream from mTOR causing epileptogenesis are poorly understood. The results from the present study suggest that inflammatory processes may represent downstream mTOR-mediated mechanisms that contribute to epileptogenesis in our mouse model of TSC. There is substantial evidence for interactions between the mTOR pathway and inflammatory mechanisms in the periphery (Weichhart and Saemann, 2009), but much less is known about this relationship in innate brain immunity.

The role of brain inflammation in the pathophysiology of various types of epilepsy has received increasing attention, especially in response to epileptogenic brain injuries (Vezzani et al., 2013a, 2013b; Xu et al., 2013). Different inflammatory mediators and pathways, such as cytokines and chemokines, are activated in a variety of animal models of epilepsy, including chemoconvulsant and electrical kindling models of epilepsy, as well as in human tissue obtained from epilepsy patients, such as with mesial temporal sclerosis (De Simoni et al., 2000; Fabene et al., 2010; Li et al., 2011; Ravizza et al., 2008a). Furthermore, anti-inflammatory treatments targeting these pathways have begun to be explored. For example, selective pharmacological inhibition of the cytokine IL-1 $\beta$  production in astrocytes inhibits seizures in rats (Maroso et al., 2011; Ravizza et al., 2008b). Although similar inflammatory markers have also been found in tubers from TSC patients (Boer et al., 2008, 2010; Maldonado et al., 2003; Prabowo et al., 2013), the pathophysiological significance of

inflammation in TSC, such as for epilepsy, is unknown. The findings from our mouse study support a potential pathogenic role of specific cytokines and chemokines in TSC. These cytokines and chemokines, such as IL-1 $\beta$  and CXCL10, may directly regulate neuronal excitability and other processes involved in epileptogenesis (Fabene et al., 2010; Li et al., 2011). As ECG, an inhibitor of IL-1 $\beta$  and CXCL10, could reduce seizures and prolong survival in *Tsc1*<sup>GFAP</sup>CKO mice, this suggests that these inflammatory processes, at least partially, contribute to epileptogenesis in these mice. Furthermore, the reversal of these inflammatory mediators by rapamycin indicates that cytokine and chemokine signaling is downstream from mTORC1 and may partially account for the antiepileptogenic effects of mTORC1 inhibition previously reported in *Tsc1*<sup>GFAP</sup>CKO mice (Zeng et al., 2008). The possibility that ECG could have other off-target effects is a limitation of this study and should be further evaluated by additional pharmacological and genetic approaches manipulating cytokine and chemokine signaling. However, ECG does not appear to directly inhibit mTOR activity (Zhang and Wong, unpublished data), indicating that its effects in *Tsc1*<sup>GFAP</sup>CKO mice are mediated by mechanisms independent of, or more likely, downstream from mTOR.

Many inflammatory reactions in the brain, such as in the cytokine system, appear to be most closely associated with glial cells, including reactive astrocytes and activated microglia. Our data indicate that at least IL-1 $\beta$  activation occurs predominantly in astrocytes from *Tsc1*<sup>GFAP</sup>CKO mice. Previous studies have demonstrated a number of cellular and molecular abnormalities in astrocytes that contribute to epileptogenesis in these mice (Jansen et al., 2005; Uhlmann et al., 2002; Wong et al., 2003; Xu et al., 2009). Thus, the current findings suggest that innate immunity or inflammatory mechanisms specifically in glia may mediate and coordinate epileptogenic mechanisms in TSC and support the recent trend emphasizing the novel role of non-neuronal cells in epilepsy. Future studies using additional cell-targeted manipulations can help define the contribution of different brain cell types in mediating inflammatory responses and epileptogenesis in TSC.

In addition to innate immunity within the brain, systemic inflammation and associated breakdown of the blood-brain barrier has also been strongly implicated in some forms of epilepsy (Kim et al., 2012; Marchi et al., 2012; Riazi et al. 2010). For example, status epilepticus and other acquired brain injuries that lead to epilepsy may elicit systemic inflammatory mechanisms, including cytokines, which lead to breakdown of the blood-brain barrier (Marchi et al., 2009). This breakdown of the blood brain barrier can lead to infiltration of pathogenic systemic inflammatory mediators, immune cells or other toxic substances into the brain that may promote epileptogenesis (Fabene et al., 2008; Ivens et al., 2007). In fact, astrocytic proteins may be involved in triggering peripheral immune responses in the context of brain injury and blood brain barrier breakdown (Bargerstock et al. 2014; Marchi et al. 2013; Zhang et al. 2014). In contrast to epilepsy related to acquired brain injuries, much less is known about a potential role of systemic inflammation in genetic epilepsies such as TSC. Despite the presence of brain inflammation in *Tsc1*<sup>GFAP</sup>CKO mice, we did not find any concurrent evidence of peripheral inflammation, suggesting that systemic inflammation is not directly involved in epileptogenesis in these mice. The importance of innate brain immunity in *Tsc1*<sup>GFAP</sup>CKO mice is further supported by the

finding of inflammatory changes in astrocyte culture and their reversal by rapamycin in vitro. Future studies can further address whether there is any evidence of blood brain barrier breakdown in these mice.

Limitations of this study include uncertainties about the causative role of inflammatory mechanisms in epileptogenesis. Based on the timing of cytokine and chemokine elevation occurring before onset of epilepsy, as well as similar findings in vitro, the inflammation changes appear to be primary events that may contribute to epileptogenesis, not secondary to seizures. However, most of this data are simply correlative. Again, the effect of ECG in the *Tsc1<sup>GFAP</sup>CKO* mice suggests that inflammatory mechanisms do contribute to the neurological phenotype of these mice, but need to be replicated with other anti-inflammatory treatments. In terms of the translational application of these findings, *Tsc1<sup>GFAP</sup>CKO* mice have some limitations in not fully recapitulating human TSC, in particular focal tuber-like lesions. As there are now a number of TSC mouse models available, examining inflammation in other brain-targeted TSC models is indicated.

Finally, this pre-clinical study provides initial proof-of-concept supporting potential translational applications of anti-inflammatory treatments for neurological manifestations of TSC. mTOR inhibitors are already being tested in clinical trials as treatments for epilepsy and cognitive deficits in TSC patients (Krueger et al., 2013). However, mTOR inhibitors potentially have significant side effects, such as immunosuppression and inhibition of mechanisms of normal growth, development, and learning. Thus, targeting mechanisms downstream from mTOR may maintain efficacy but reduce side effects. Anti-inflammatory drugs may represent rational candidates for developing novel antiepileptogenic or antiseizure treatments for TSC.

In summary, this study identifies inflammatory mechanisms involving specific cytokines and chemokines which are abnormally activated in a mouse model of TSC. Inhibition of these mechanisms was associated with a decrease in seizures and improved survival in these mice, providing proof-of-concept that anti-inflammatory treatments represent potential therapy for this genetic epilepsy.

## Supplementary Material

Refer to Web version on PubMed Central for supplementary material.

## Acknowledgments

This work was supported by grants from the National Institutes of Health (R01 NS056872 to MW and S10 RR027552 to Washington University) and the Department of Defense (W81XWH-12-1-0190 to MW), and by the Alafi Neuroimaging Lab at Washington University.

## ABBREVIATIONS

<b>ANOVA</b>	analysis of variance
<b>CKO</b>	conditional knock-out

<b>ECG</b>	epicatechin-3-gallate
<b>EEG</b>	electroencephalography
<b>GFAP</b>	glial fibrillary acidic protein
<b>IL-1 <math>\beta</math></b>	interleukin-1 $\beta$
<b>KO</b>	knock-out
<b>mTOR</b>	mammalian target of rapamycin
<b>mTORC1</b>	mammalian target of rapamycin complex 1
<b>RT-PCR</b>	reverse transcriptase polymerase chain reaction
<b>SEGA</b>	subependymal giant cell astrocytoma
<b>TSC</b>	tuberous sclerosis complex

## References

- Bargerstock E, Puvenna V, Iffland P, Falcone T, Hossain M, Vetter S, Man S, Dickstein L, Marchi N, Ghosh C, Carvalho-Tavares J, Janigro D. Is peripheral immunity regulated by blood-brain barrier permeability changes? *PLoS One*. 2014; 9:e101477. [PubMed: 24988410]
- Berdichevsky Y, Dryer AM, Saponijian Y, Mahoney MM, Pimentel CA, Lucini CA, Usenovic M, Staley KJ. PI3K-Akt signaling activates mTOR-mediated epileptogenesis in organotypic hippocampal culture model of post-traumatic epilepsy. *J Neurosci*. 2013; 33:9056–9067. [PubMed: 23699517]
- Boer K, Jansen F, Nellist M, Redeker S, van den Ouweland AM, Spliet WG, van Nieuwenhuizen O, Troost D, Crino PB, Aronica E. Inflammatory processes in cortical tubers and subependymal giant cell tumors of tuberous sclerosis complex. *Epilepsy Res*. 2008; 78:7–21. [PubMed: 18023148]
- Boer K, Crino PB, Gorter JA, Nellist M, Jansen FE, Spliet WG, van Rijen PC, Wittink FR, Breit TM, Troost D, Wadman WJ, Aronica E. Gene expression analysis of tuberous sclerosis complex cortical tubers reveals increased expression of adhesion and inflammatory factors. *Brain Pathol*. 2010; 20:704–719. [PubMed: 19912235]
- Chu-Shore CJ, Major P, Camposano S, Muzykewicz D, Thiele E. The natural history of epilepsy in tuberous sclerosis complex. *Epilepsia*. 2010; 51:1236–1241. [PubMed: 20041940]
- Crino PB, Nathanson KL, Henske EP. The tuberous sclerosis complex. *N Engl J Med*. 2006; 355:1345–1356. [PubMed: 17005952]
- Crouvezier S, Powell B, Keir D, Yaqoob P. The effects of phenolic components of tea on the production of pro- and anti-inflammatory cytokines by human leukocytes in vitro. *Cytokine*. 2001; 13:280–286. [PubMed: 11243706]
- De Simoni MG, Perego C, Ravizza T, Moneta D, Conti M, Marchesi F, De Luigi A, Garattini S, Vezzani A. Inflammatory cytokines and related genes are induced in the rat hippocampus by limbic status epilepticus. *Eur J Neurosci*. 2000; 12:2623–2633. [PubMed: 10947836]
- Erbayat-Altay E, Zeng LH, Xu L, Gutmann D, Wong M. The natural history and treatment of epilepsy in a murine model of tuberous sclerosis. *Epilepsia*. 2007; 48:1470–1476. [PubMed: 17484760]
- Fabene PF, Bramanti P, Constantin G. The emerging role for chemokines in epilepsy. *J Neuroimmunol*. 2010; 224:22–27. [PubMed: 20542576]
- Fabene PF, Navarro Mora G, Martinello M, Rossi B, Merigo F, Ottoboni L, Bach S, Angiari S, Benati D, Chakir A, Zanetti L, Schio F, Osculati A, Marzola P, Nicolato E, Homeister JW, Xia L, Lowe JB, McEver RP, Osculati F, Sbarbati A, Butcher EC, Constantin G. A role for leukocyte-endothelial adhesion mechanisms in epilepsy. *Nat Med*. 2008; 14:1377–1383. [PubMed: 19029985]

- Franz DN, Belousova E, Sparagana S, Bebin EM, Frost M, Kuperman R, Witt O, Kohrman MH, Flamini JR, Wu JY, Curatolo P, de Vries PJ, Whittemore VH, Thiele EA, Ford JP, Shah G, Cauwel H, Lebowitz D, Sahnoud T, Jozwiak S. Efficacy and safety of everolimus for subependymal giant cell astrocytomas associated with tuberous sclerosis complex (EXIST-1): a multicentre, randomized, placebo-controlled phase 3 trial. *Lancet*. 2013; 381:125–132. [PubMed: 23158522]
- Goto J, Talos DM, Klein P, Qin W, Chekaluk YI, Anderl S, Malinowska IA, Di Nardo A, Bronson RT, Chan JA, Vinters HV, Kernie SG, Jensen FE, Sahin M. Regulable neural progenitor-specific *TSC1* loss yields giant cells with organellar dysfunction in a model of tuberous sclerosis complex. *Proc Natl Acad Sci USA*. 2011; 108:1070–1079. [PubMed: 21199944]
- Guo DG, Zeng LH, Brody DL, Wong M. Rapamycin attenuates the development of posttraumatic epilepsy in a mouse model of traumatic brain injury. *PLoS One*. 2013; 8:e64078. [PubMed: 23691153]
- Holmes GL, Stafstrom CE. the Tuberous Sclerosis Study Group. Tuberous Sclerosis Complex and epilepsy: recent developments and future challenges. *Epilepsia*. 2007; 48:617–630. [PubMed: 17386056]
- Hosokawa Y, Hosokawa I, Ozaki K, Nakanishi T, Nakae H, Matsuo T. Catechins inhibit CXCL10 production from oncostatin M-stimulated human gingival fibroblasts. *J Nutr Biochem*. 2010; 21:659–664. [PubMed: 19616927]
- Huang X, Zhang H, Yang J, Wu J, McMahon J, Lin Y, Cao Z, Gruenthal M, Huang Y. Pharmacological inhibition of the mammalian target of rapamycin pathway suppresses acquired epilepsy. *Neurobiol Dis*. 2010; 40:193–199. [PubMed: 20566381]
- Ivens S, Kaufer D, Flores LP, Bechmann I, Zumsteg D, Tomkins O, Seiffert E, Heinemann U, Friedman A. TFG-beta receptor-mediated albumin uptake into astrocytes is involved in neocortical epileptogenesis. *Brain*. 2007; 130:535–547. [PubMed: 17121744]
- Jansen LA, Uhlmann EJ, Gutmann DH, Wong M. Epileptogenesis and reduced inward rectifier potassium current in *Tuberous Sclerosis Complex-1* deficient astrocytes. *Epilepsia*. 2005; 46:1871–1880. [PubMed: 16393152]
- Kim SY, Buckwalter M, Soreq H, Vezzani A, Kaufer D. Blood-brain barrier dysfunction-induced inflammatory signaling in brain pathology and epileptogenesis. *Epilepsia*. 2012; 53(Suppl 6):37–44. [PubMed: 23134494]
- Krueger DA, Care MM, Holland K, Agricola K, Tudor C, Mangeshkar P, Wilson KA, Byars A, Sahnoud T, Franz DN. Everolimus for subependymal giant-cell astrocytomas in Tuberous Sclerosis. *N Engl J Med*. 2010; 363:1801–1811. [PubMed: 21047224]
- Krueger DA, Wilfong AA, Holland-Bouley K, Anderson AE, Agricola K, Tudor C, Mays M, Lopez CM, Kim MO, Franz DN. Everolimus treatment of refractory epilepsy in tuberous sclerosis complex. *Ann Neurol*. 2013; 74:679–687. [PubMed: 23798472]
- Li G, Bauer S, Nowak M, Norwood B, Tackenberg B, Rosenow F, Knake S, Oertel WH, Hamer HM. Cytokines and epilepsy. *Seizure*. 2011; 20:249–256. [PubMed: 21216630]
- Maldonado M, Baybis M, Newman D, Kolson DL, Chen W, McKhann G, Gutmann DH, Crino PB. Expression of ICAM-1, TNF- $\alpha$ , NF $\kappa$ B, and MAP kinase in tubers of the tuberous sclerosis complex. *Neurobiol Dis*. 2003; 14:279–290. [PubMed: 14572449]
- Marchi N, Bazarian JJ, Puvenna V, Janigro M, Ghosh C, Zhong J, Zhu T, Blackman E, Stewart D, Ellis J, Butler R, Janigro D. Consequences of repeated blood-brain barrier disruption in football players. *PLoS One*. 2013; 8:e56805. [PubMed: 23483891]
- Marchi N, Fan Q, Ghosh C, Fazio V, Berolini F, Betto G, Batra A, Carlton E, Najm I, Granata T, Janigro D. Antagonism of peripheral inflammation reduces the severity of status epilepticus. *Neurobiol Dis*. 2009; 33:171–181. [PubMed: 19010416]
- Marchi N, Granatam T, Ghosh C, Janigro D. Blood-brain barrier dysfunction and epilepsy: pathophysiologic roles and therapeutic approaches. *Epilepsia*. 2012; 53:1877–1886. [PubMed: 22905812]
- Maroso M, Balosso S, Ravizza T, Liu J, Bianchi ME, Vezzani A. Interleukin-1 $\beta$  biosynthesis inhibition reduces acute seizures and drug resistant chronic epileptic activity in mice. *Neurotherapeutics*. 2011; 8:304–315. [PubMed: 21431948]

- Meikle L, Pollizzi K, Egnor A, Kramvis I, Lane H, Sahin M, Kwiatkowski DJ. Response of a neuronal model of Tuberous Sclerosis to mammalian target of Rapamycin (mTOR) inhibitors: effects on mTORC1 and Akt signaling lead to improved survival and function. *J Neurosci*. 2008; 28:5422–5432. [PubMed: 18495876]
- Orlova KA, Crino PB. The tuberous sclerosis complex. *Ann NY Acad Sci*. 2010; 1184:87–105. [PubMed: 20146692]
- Prabowo AS, Anink JJ, Lammens M, Mellist M, van den Ouweland AM, Adle-Biassette H, Sarnat HB, Flores-Sarnat L, Crino PB, Aronica E. Fetal brain lesions in tuberous sclerosis complex: TORC1 activation and inflammation. *Brain Pathol*. 2013; 23:45–59. [PubMed: 22805177]
- Ravizza T, Boer K, Redeker S, Spliet WGM, van Rijen PC, Troost D, Vezzani A, Aronica E. The IL-1 $\beta$  system in epilepsy-associated malformations of cortical development. *Neurobiol Dis*. 2006; 24:128–143. [PubMed: 16860990]
- Ravizza T, Gagliardi B, Noe F, Boer K, Aronica E, Vezzani A. Innate and adaptive immunity during epileptogenesis and spontaneous seizures: evidence from experimental models and human temporal lobe epilepsy. *Neurobiol Dis*. 2008a; 29:142–160. [PubMed: 17931873]
- Ravizza T, Noe F, Zardoni D, Vaghi V, Sifringer M, Vezzani A. Interleukin converting enzyme inhibition impairs kindling epileptogenesis in rats by blocking astrocytic IL-1 $\beta$  production. *Neurobiol Dis*. 2008b; 31:327–333. [PubMed: 18632279]
- Riazi K, Galic MA, Pitmann QJ. Contributions of peripheral inflammation to seizure susceptibility: cytokines and brain excitability. *Epilepsy Res*. 2010; 89:34–43. [PubMed: 19804959]
- Uhlmann EJ, Wong M, Baldwin RL, Bajenaru ML, Onda H, Kwiatkowski DJ, Yamada KA, Gutmann DH. Astrocyte-specific TSC1 conditional knockout mice exhibit abnormal neuronal organization and seizures. *Ann Neurol*. 2002; 52:285–296. [PubMed: 12205640]
- van Vliet EA, Forte G, Holtman L, den Burger JC, Sinjewel A, de Vries HE, Aronica E, Gorter JA. Inhibition of mammalian target of rapamycin reduces epileptogenesis and blood-brain barrier leakage but not microglia activation. *Epilepsia*. 2012; 53:1254–1263. [PubMed: 22612226]
- Vezzani A, Aronica E, Mazarati A, Pittman QJ. Epilepsy and brain inflammation. *Exp Neurol*. 2013a; 244:11–21. [PubMed: 21985866]
- Vezzani A, Friedman A, Dingledine RJ. The role of inflammation in epileptogenesis. *Neuropharmacology*. 2013b; 69:16–24. [PubMed: 22521336]
- Xu D, Miller SD, Koh S. Immune mechanisms in epileptogenesis. *Front Cell Neurosci*. 2013; 7:195. [PubMed: 24265605]
- Xu L, Zeng LH, Wong M. Impaired astrocyte gap junction coupling and potassium buffering in a mouse model of Tuberous Sclerosis Complex. *Neurobiol Dis*. 2009; 34:291–299. [PubMed: 19385061]
- Weicchart T, Saemann MD. The multiple facets of mTOR in immunity. *Trends Immunol*. 2009; 30:218–226. [PubMed: 19362054]
- Wong M. Mechanisms of epileptogenesis in tuberous sclerosis complex and related malformations of cortical development with abnormal glioneuronal proliferation. *Epilepsia*. 2008; 49:8–21. [PubMed: 17727667]
- Wong M. Mammalian target of rapamycin (mTOR) inhibition as potential antiepileptogenic therapy: from tuberous sclerosis to common acquired epilepsies. *Epilepsia*. 2010; 51:27–36. [PubMed: 19817806]
- Wong M. A critical review of mTOR inhibitors and epilepsy: from basic science to clinical trials. *Expert Rev Neurotherap*. 2013; 13:657–669.
- Wong M, Ess KE, Uhlmann EJ, Jansen LA, Li W, Crino PB, Mennerick S, Yamada KA, Gutmann DH. Impaired astrocyte glutamate transport in a mouse epilepsy model of tuberous sclerosis complex. *Ann Neurol*. 2003; 54:251–256. [PubMed: 12891680]
- Zeng LH, Xu L, Gutmann DH, Wong M. Rapamycin prevents epilepsy in a mouse model of tuberous sclerosis complex. *Ann Neurol*. 2008; 63:444–453. [PubMed: 18389497]
- Zeng LH, Rensing NR, Wong M. The mammalian target of rapamycin signaling pathway mediates epileptogenesis in a model of temporal lobe epilepsy. *J Neurosci*. 2009; 29:6964–72. [PubMed: 19474323]

- Zeng L, Rensing NR, Zhang B, Gutmann DH, Gambello MJ, Wong M. *TSC2* gene inactivation causes a more severe epilepsy phenotype than *TSC1* inactivation in a mouse model of Tuberous Sclerosis Complex. *Hum Mol Genet.* 2011; 20:445–454. [PubMed: 21062901]
- Zhang B, Yang L, Konishi Y, Maeda N, Sakanaka M, Tanaka J. Suppressive effects of phosphodiesterase type IV inhibitors on rat cultured microglial cells: comparison with other types of cAMP-elevating agents. *Neuropharm.* 2002; 42:262–269.
- Zhang Z, Zoltewicz JS, Mondello S, Newsom KJ, Yang Z, Yang B, Kobeissay F, Guingab J, Glushakova O, Robicsek S, Heaton S, Buki A, Hannay J, Gold MS, Rubenstein R, Lu XC, Dave JR, Schmid K, Tortella F, Robertson CS, Wang KK. Human traumatic brain injury induces autoantibody response against glial fibrillary acidic protein and its breakdown products. *PLoS One.* 2014; 9:e92698. [PubMed: 24667434]

### Highlights

- Cytokines and chemokines are activated in a mouse model of tuberous sclerosis.
- An antiinflammatory agent, epicatechin, decreases seizures and prolongs survival in this model.
- This study implicates inflammatory mechanisms in contributing to a genetic epilepsy.



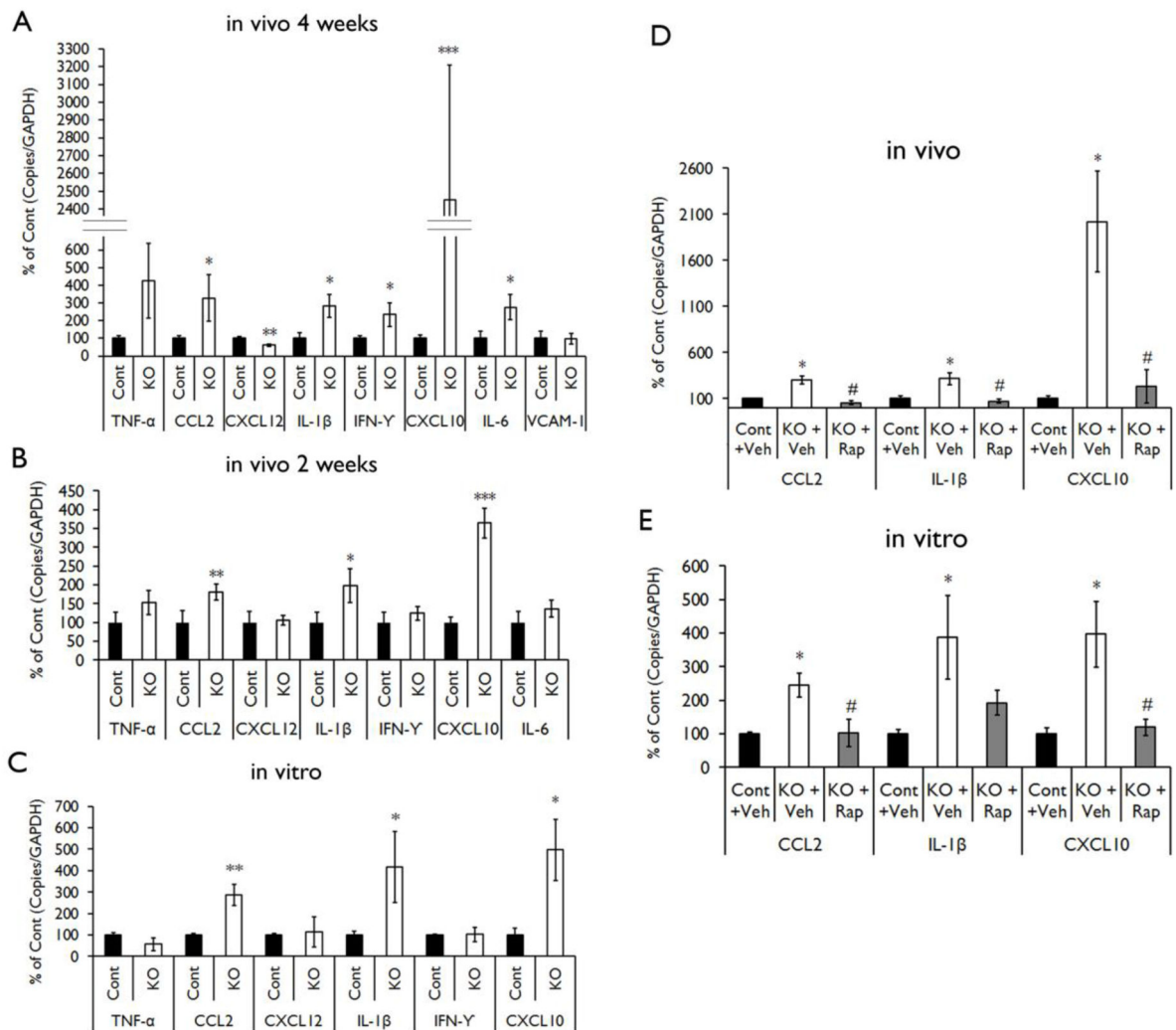


**Figure 1. Proinflammatory cytokines and chemokines are up-regulated in *Tsc1*<sup>GFAP</sup>CKO mice and inhibited by rapamycin**

mRNA expression of cytokines and chemokines was evaluated by real-time quantitative RT-PCR in the brains or cultured astrocytes from *Tsc1*<sup>GFAP</sup>CKO and control mice. (A) The mRNA levels of CCL2, IL-1 $\beta$ , IFN- $\gamma$ , CXCL10 and IL-6 were increased in four-week old *Tsc1*<sup>GFAP</sup>CKO mice compared with control mice, but CXCL12 was decreased (n = 8–10 mice/group). (B) The mRNA levels of CCL2, IL-1 $\beta$  and CXCL10 were increased in two-week old *Tsc1*<sup>GFAP</sup>CKO mice compared with control mice (n = 8–11 mice/group). (C) The mRNA levels of CCL2, IL-1 $\beta$  and CXCL10 were increased in cultured astrocytes from *Tsc1*<sup>GFAP</sup>CKO mice compared with astrocytes from control mice (n = 5–9 mice/group). \* p < 0.05, \*\* p < 0.01, \*\*\* p < 0.001, versus control mice by Student's *t* test. (D) Seven days of rapamycin treatment (3 mg/kg/d i.p.) significantly inhibited the mRNA levels of CCL2, IL-1 $\beta$  and CXCL10 in the brains of *Tsc1*<sup>GFAP</sup>CKO mice compared with vehicle-treated *Tsc1*<sup>GFAP</sup>CKO mice (n = 4–12 mice/group). (E) Rapamycin treatment (2 ng/ml for 16 hours) significantly inhibited the mRNA levels of CCL2 and CXCL10, but not IL-1 $\beta$ , in cultured astrocytes from *Tsc1*<sup>GFAP</sup>CKO mice (n = 5–12 mice/group). \* p < 0.05 versus

control mice, #  $p < 0.05$  versus vehicle-treated  $Tsc1^{GFAP}CKO$  mice by one-way ANOVA.  
Cont = control mice, KO =  $Tsc1^{GFAP}CKO$ , Veh = vehicle, Rap = Rapamycin.

Author Manuscript

Author Manuscript

Author Manuscript

Author Manuscript

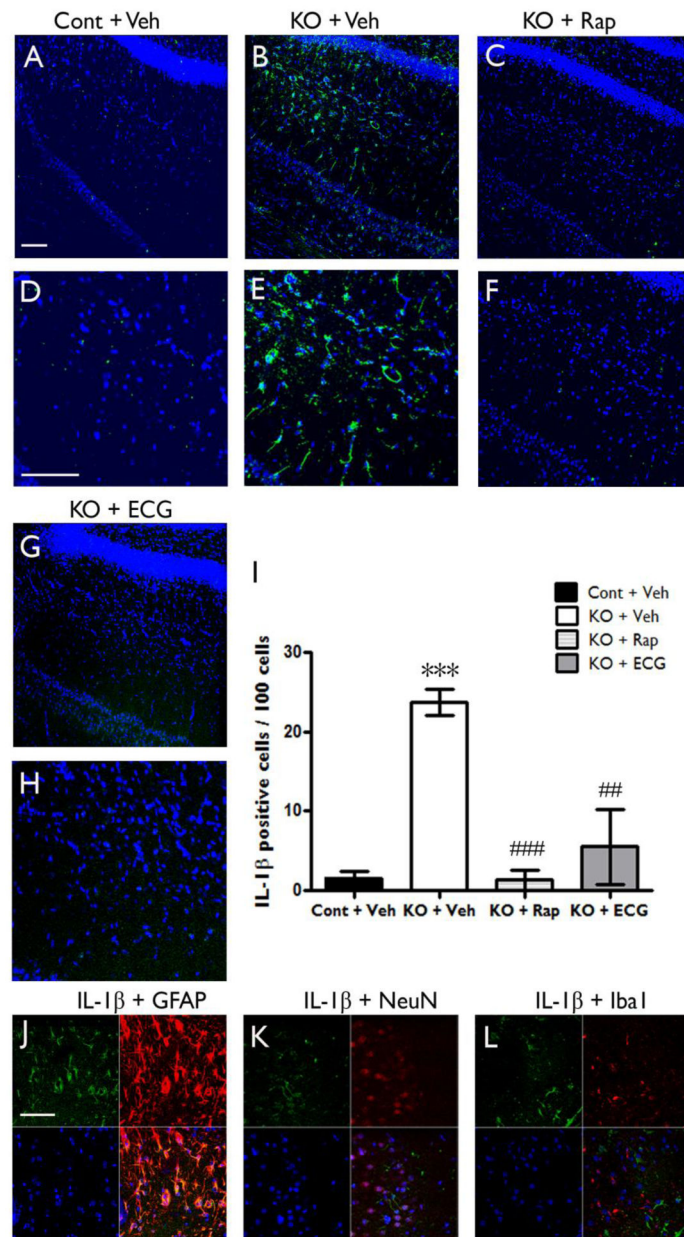


**Figure 2. IL-1 $\beta$  protein is upregulated in *Tsc1*<sup>GFAP</sup>CKO mice and inhibited by anti-inflammatory treatments**

Protein expression of IL-1 $\beta$  was assessed by immunohistochemistry in *Tsc1*<sup>GFAP</sup>CKO and control mice, as well as in rapamycin or ECG treated *Tsc1*<sup>GFAP</sup>CKO mice. (A–H) Confocal images of immunohistochemical staining of IL-1 $\beta$  (green) and TO-PRO-3 Iodide (blue). TO-PRO-3 Iodide (blue) was used as an optimal fluorescence dye for nuclear counterstaining. IL-1 $\beta$  protein expression was detected in brain sections of *Tsc1*<sup>GFAP</sup>CKO mice (B,E KO + Veh), but not in control mice (A,D Cont + Veh). Rapamycin (C,F KO + Rap) and ECG (G,H KO + ECG) treatment inhibited the IL-1 $\beta$  expression. Scale bars = 100  $\mu$ m. (I) Quantitative analysis confirmed an increase in IL-1 $\beta$ -positive cells (per 100 TO-PRO-3 positive cells) in vehicle-treated *Tsc1*<sup>GFAP</sup>CKO group (KO + Veh) compared with vehicle-treated control

group (Cont + Veh). Rapamycin (3 mg/kg/d i.p. for one week) or ECG treatment (12.5 mg/kg/d i.p. for one week) significantly decreased IL-1 $\beta$ -positive cells. \*\*\*p<0.05 versus vehicle-treated control mice (n=4–5 mice/group); ## p<0.01, ### p<0.001 versus vehicle-treated *Tsc1*<sup>GFAP</sup>CKO mice by two-way ANOVA. (J, K, L) Double label immunofluorescence confocal microscopy for expression of IL-1 $\beta$  protein (green) with GFAP (F, red for astrocytes), NeuN (G, red for neurons) and Iba1 (H, red for microglia) within brain sections of four-week-old *Tsc1*<sup>GFAP</sup>CKO mice. All sections were also labeled with TO-PRO-3 Iodide (blue) as an optimal fluorescence dye for nuclear counterstaining. IL-1 $\beta$  was found co-localized with GFAP, but not with NeuN and Iba1. Scale bar = 50  $\mu$ m. Cont = control, KO = *Tsc1*<sup>GFAP</sup>CKO, TO PRO3 = TO-PRO-3 Iodide, ECG = Epicatechin-3-gallate, Rap = Rapamycin.

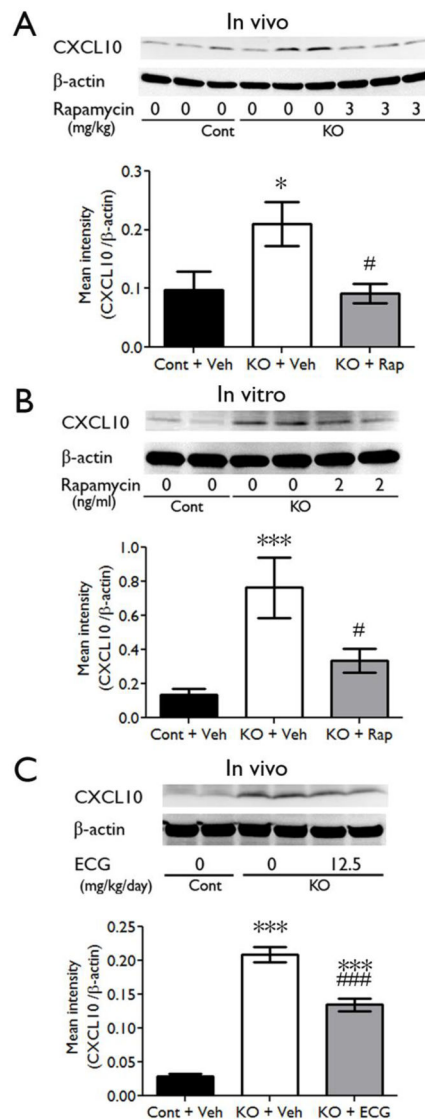


**Figure 3. CXCL10 protein is upregulated in *Tsc1*<sup>GFAP</sup>CKO mice and reversed by anti-inflammatory treatment in vivo and in vitro**

Protein expression of CXCL10 was assessed by western blotting in the brains and cultured astrocytes of *Tsc1*<sup>GFAP</sup>CKO mice, and the effects of rapamycin and ECG were tested. (A) Vehicle-treated *Tsc1*<sup>GFAP</sup>CKO mice have significantly increased CXCL10 levels, compared with control mice. Rapamycin treatment (3 mg/kg/d i.p. for seven days) significantly inhibited the upregulated-CXCL10 in *Tsc1*<sup>GFAP</sup>CKO mice (7–11 mice/group). (B) Vehicle-treated cultured astrocytes from *Tsc1*<sup>GFAP</sup>CKO mice showed increased CXCL10 expression compared with astrocytes from control mice. Rapamycin treatment (2 ng/ml added to the culture medium for 16 hours) blocked the up-regulation of CXCL10 in *Tsc1*<sup>GFAP</sup>CKO astrocyte (n=8–12 mice/group). (C) Vehicle-treated *Tsc1*<sup>GFAP</sup>CKO mice have significantly increased CXCL10 protein expression compared with control mice. ECG treatment (12.5 mg/kg/d i.p. for seven days) inhibited the increased CXCL10 in *Tsc1*<sup>GFAP</sup>CKO mice, but this was still significantly higher than control mice (n=8 mice/group). \* p<0.05, \*\*\*

p<0.001, versus vehicle-treated control mice or astrocytes by one-way ANOVA; # p<0.05, ### p<0.001, versus vehicle-treated *Tsc1*<sup>GFAP</sup>CKO mice or astrocytes by one-way ANOVA (n = 9–12 mice/group). Cont = control, KO = *Tsc1*<sup>GFAP</sup>CKO, Veh = vehicle, Rap = Rapamycin, ECG = Epicatechin-3-gallate.

Author Manuscript

Author Manuscript

Author Manuscript

Author Manuscript

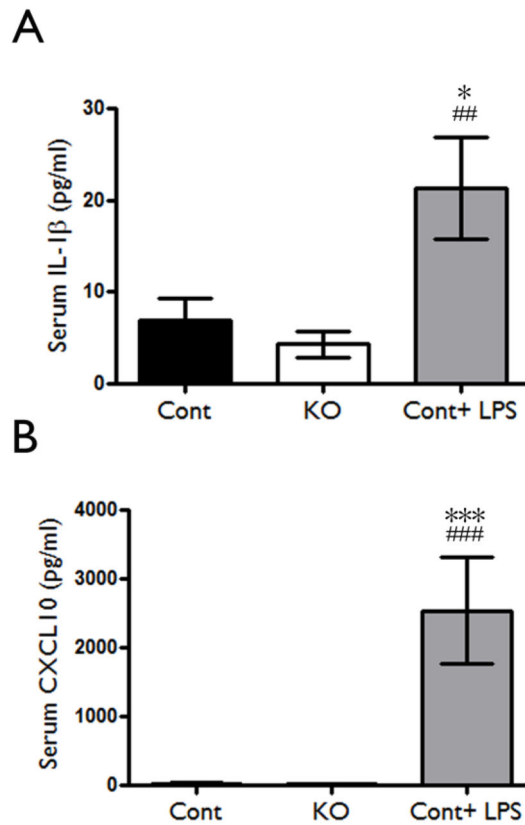


**Figure 4. Lack of evidence for systemic inflammation in *Tsc1*<sup>GFAP</sup>CKO mice**

Serum inflammatory markers were assessed in *Tsc1*<sup>GFAP</sup>CKO mice to evaluate the potential involvement of the peripheral immune system in contributing to brain inflammation. There was no significant difference in serum IL-1 $\beta$  (A) and CXCL10 (B) protein levels as assayed by ELISA in 4 week-old *Tsc1*<sup>GFAP</sup>CKO mice compared with control mice, while LPS induced a significant increase in these markers in control mice. \*  $p < 0.05$ , \*\*\*  $p < 0.001$ , versus vehicle-treated control mice by one-way ANOVA; ##  $p < 0.01$ , ###  $p < 0.001$ , versus vehicle-treated *Tsc1*<sup>GFAP</sup>CKO mice by one-way ANOVA ( $n = 5-9$  mice/group). Cont = control, KO = *Tsc1*<sup>GFAP</sup>CKO.

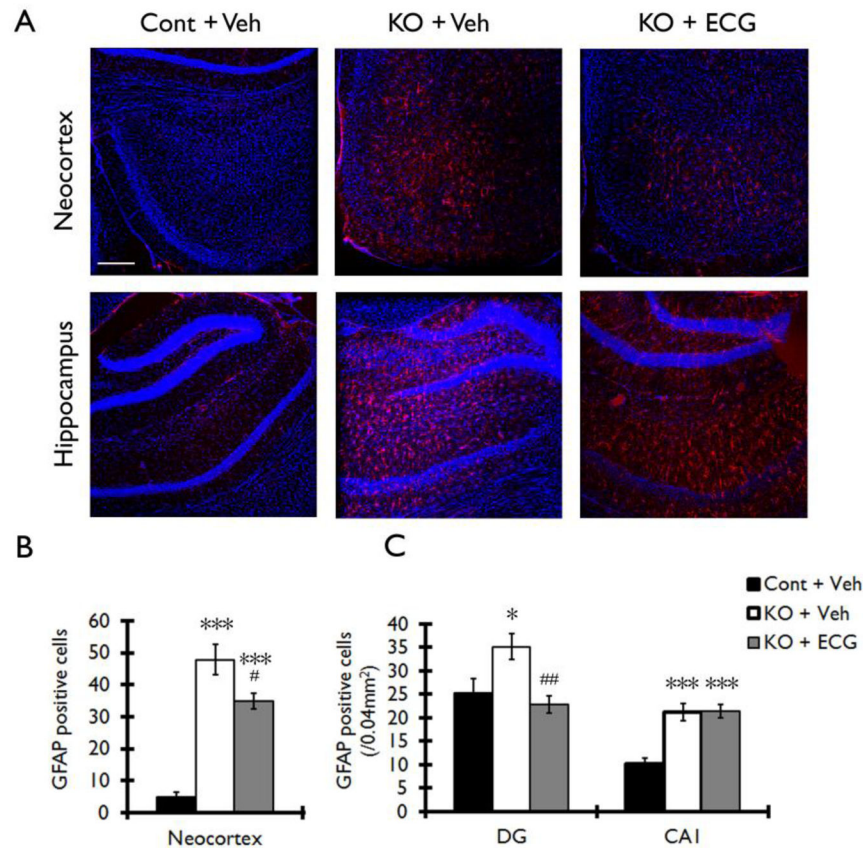


**Figure 5. ECG treatment decreases the number of GFAP positive cells in neocortex and hippocampus of *Tsc1*<sup>GFAP</sup>CKO mice**

The effect of ECG on the number of GFAP positive cells was assessed in *Tsc1*<sup>GFAP</sup>CKO mice by immunohistochemistry. (A) Vehicle-treated *Tsc1*<sup>GFAP</sup>CKO mice (KO + Veh) displayed a diffuse increase in GFAP-positive cells (red) in neocortex (upper middle panel) and hippocampus (lower middle panel) compared with the vehicle-treated control mice (Cont + Veh). ECG treatment partially prevented this increase in GFAP-positive cells in *Tsc1*<sup>GFAP</sup>CKO mice (KO + ECG). TO-PRO-3 Iodide (blue) was used as an optimal fluorescence dye for nuclear counterstaining. (B, C) Quantitative analysis confirmed an increase in GFAP-positive cells in vehicle-treated *Tsc1*<sup>GFAP</sup>CKO group (KO + Veh) compared with vehicle-treated control group (Cont + Veh) in neocortex, dentate gyrus (DG) and CA1 of hippocampus. ECG treatment (12.5 mg/kg/d i.p. for four weeks) decreased GFAP-positive cells in neocortex and DG, but not in CA1 (KO + ECG; n=8 mice/group). \*p<0.05, \*\*\* p<0.001 versus vehicle-treated control mice by two-way ANOVA; #p<0.05, ## p<0.01 versus vehicle-treated *Tsc1*<sup>GFAP</sup>CKO mice by two-way ANOVA. Scale bar = 200  $\mu$ m. Cont = control mice, KO = *Tsc1*<sup>GFAP</sup>CKO mice, Veh = vehicle, ECG = Epicatechin-3-gallate, DG = dentate gyrus, CA1 = CA1 pyramidal cell layer of hippocampus.



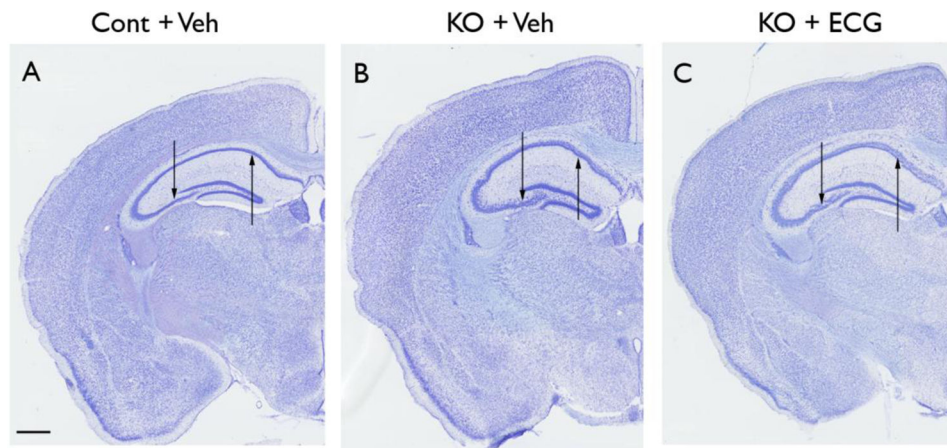


**Figure 6. ECG treatment does not prevent neuronal disorganization in *Tsc1*<sup>GFAP</sup>CKO mice**  
 The effect of ECG on neuronal organization was assessed in *Tsc1*<sup>GFAP</sup>CKO mice by cresyl violet staining. Compared with control mice (A), vehicle-treated *Tsc1*<sup>GFAP</sup>CKO mice (B) exhibited widely dispersed pyramidal cell layers (arrows) in all regions of hippocampus (CA1–CA4). ECG treated *Tsc1*<sup>GFAP</sup>CKO mice (C) had a similar pattern as vehicle-treated *Tsc1*<sup>GFAP</sup>CKO group (B), with no apparent effect on this neuronal disorganization. Scale bar = 500  $\mu$ m. Cont = control mice, KO = *Tsc1*<sup>GFAP</sup>CKO mice, Veh = vehicle, ECG = Epicatechin-3-gallate.

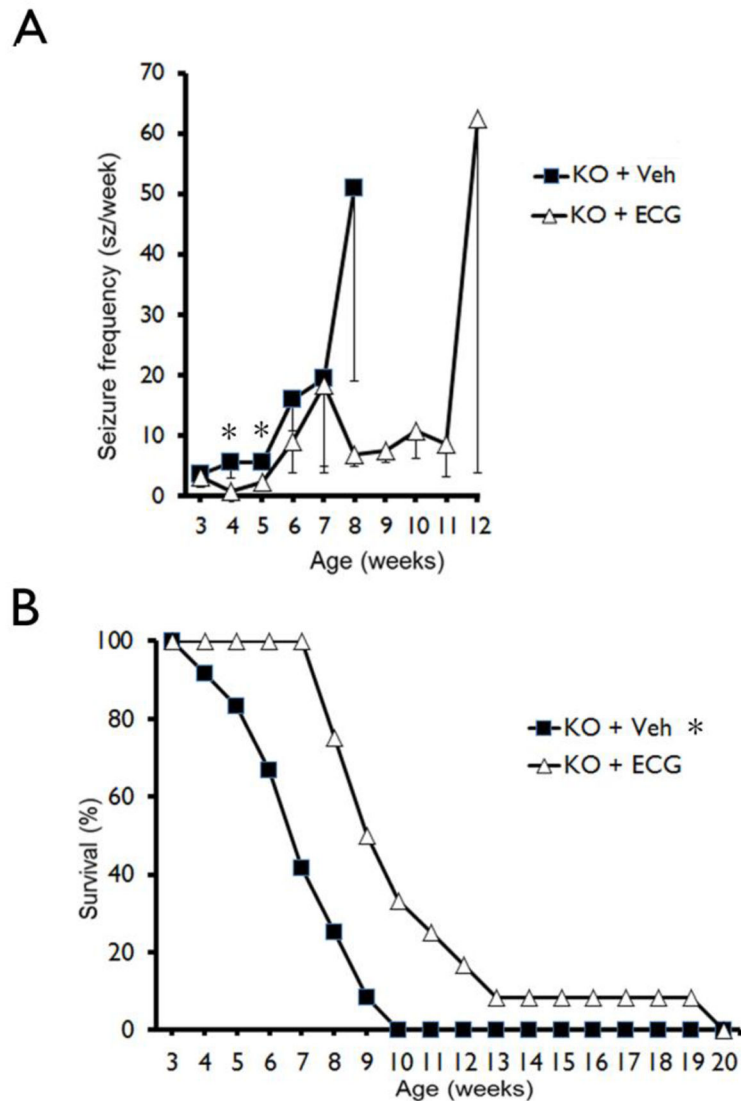


**Figure 7. ECG treatment slightly decreases the development of seizures and improves survival in *Tsc1*<sup>GFAP</sup>CKO mice**

(A) Seizures start to develop in vehicle-treated *Tsc1*<sup>GFAP</sup>CKO mice (A, KO + Veh) around 3 weeks and become progressively more frequent with age. ECG treatment (12.5 mg/kg/d i.p. starting at 3 weeks of age (KO + ECG) slightly decreased seizure frequency in *Tsc1*<sup>GFAP</sup>CKO mice at 4 and 5 weeks of age compared with vehicle-treated *Tsc1*<sup>GFAP</sup>CKO mice. (\* $p < 0.05$  by one-way ANOVA,  $n = 12$  mice/group). However, all mice were found to have at least one seizure in both vehicle-treated and ECG-treated *Tsc1*<sup>GFAP</sup>CKO mice. (B) Survival analysis showed that vehicle-treated *Tsc1*<sup>GFAP</sup>CKO mice die prematurely with 50% mortality between 6–7 weeks of age and 100% mortality by 10 weeks. ECG treatment (12.5 mg/kg/d i.p. starting at 3 weeks of age) significantly improved the survival of *Tsc1*<sup>GFAP</sup>CKO mice compared to vehicle treated *Tsc1*<sup>GFAP</sup>CKO mice, but all ECG-treated

mice still died by 20 weeks of age. \* $p < 0.05$  by Chi-Square test, comparing the two groups (n = 12 mice/group). KO = *Tsc1*<sup>GFAP</sup>CKO, Veh = vehicle, ECG = Epicatechin-3-gallate.

Author Manuscript

Author Manuscript

Author Manuscript

Author Manuscript